

Argon and Silicon abundances in the damped Ly α system I Zw 18

Sergei A. Levshakov¹, Wilhelm H. Kegel², and Irina I. Agafonova¹

¹ Department of Theoretical Astrophysics, Ioffe Physico-Technical Institute, 194021 St. Petersburg, Russia

² Institut für Theoretische Physik der Universität Frankfurt am Main, 60054 Frankfurt/Main 11, Germany

Received 00 December 2000 / Accepted 00 December 2000

Abstract. We show that the difference between the Ar and Si relative abundance ratio derived from *FUSE* absorption spectra and from the H II regions of I Zw 18 is a consequence of the microturbulent analysis applied to the absorption spectra. *FUSE* observations were performed with a large entrance aperture which fully covered the galaxy. This means that the observed profiles are averaged over the full body of I Zw 18, implying that large-scale velocity fields influence the absorption-line profiles. Taking this into account, we show that the absorption spectra are consistent with the same metal abundances as those derived from the H II regions. It follows that no significant ionization correction as suggested by Izotov and collaborators to describe metal contents in damped Ly α systems (DLA) is required to model abundances in the neutral gas of I Zw 18 (a local DLA system). Using a mesoturbulent approach and applying the generalized radiative transfer equation to the Ar I λ 1048 and Si II λ 1020 lines observed by Vidal-Madjar et al., we found that the profiles may be reproduced with $\log(\text{Ar}/\text{Si}) \simeq -0.8$ and $N(\text{Si II}) \simeq 4 \times 10^{15} \text{ cm}^{-2}$.

Key words: line: formation – line: profiles – galaxies: absorption lines – galaxies: individual: I Zw 18

1. Introduction

The blue compact galaxy (BCG) I Zw 18 (Mrk 116) has been an intensively studied object for the last three decades since the first spectroscopic observations by Zwicky (1966). I Zw 18 shows an intense and recent burst of star formation which makes this galaxy an attractive target for studies of star formation history. Recent observations revealed, for example, two stellar populations in I Zw 18: 10–20 Myr red supergiants and 0.1–5 Gyr asymptotic giant branch stars (Östlin 2000).

Amongst BCGs, I Zw 18 shows the lowest oxygen abundance: the northwest (NW) and the southeast (SE)

bright H II regions yield $\log(\text{O}/\text{H}) = -4.83 \pm 0.03$ and -4.82 ± 0.03 , respectively (Izotov et al. 1999). Relative to solar values, one finds $[\text{O}/\text{H}]^1 = -1.70 \pm 0.08$, i.e. $Z/Z_{\odot} \simeq 1/50$. For argon abundances, Izotov et al. obtained $\log(\text{Ar}/\text{H}) = -6.90 \pm 0.05$ (NW) and a slightly lower ratio for the SE region, $\log(\text{Ar}/\text{H}) = -7.23 \pm 0.05$. Silicon abundances measured by Izotov & Thuan (1999) give $\log(\text{Si}/\text{H}) = -6.29 \pm 0.22$ (NW) and $\log(\text{Si}/\text{H}) = -6.30 \pm 0.22$ (SE). Thus, these values imply for the NW emission patch $[\text{Ar}/\text{H}] = -1.42 \pm 0.06$ and $[\text{Si}/\text{H}] = -1.85 \pm 0.22$.

The neutral gas properties in I Zw 18 have been probed in both the radio (see van Zee et al. 1998 and references cited therein) and the UV range (Kunth et al. 1994; Pettini & Lipman 1995; Vidal-Madjar et al. 2000). High velocity and high spatial resolution radio observations have shown that the overall kinematics of the H I gas associated with I Zw 18 is very complex and the neutral gas velocity dispersion σ equals $13 - 14 \text{ km s}^{-1}$, or $b \equiv \sqrt{2}\sigma = 18 - 20 \text{ km s}^{-1}$ (van Zee et al. 1998). The H I column density in front of I Zw 18 deduced from the Ly α absorption profile by Kunth et al., $N(\text{H I}) = (3.5 \pm 0.5) \times 10^{21} \text{ cm}^{-2}$, is comparable to the peak H I surface density found by van Zee et al., $N(\text{H I}) \simeq 3.0 \times 10^{21} \text{ cm}^{-2}$. This means that the neutral gas in I Zw 18 can be considered as a local damped Ly α system (DLA) which is similar to high redshift DLAs observed in the light of background quasars.

First measurement of the O/H abundance in the H I region have indicated a possible discrepancy between the metal content in the neutral gas and in the H II regions (Kunth et al. 1994). This, however, was not confirmed in later studies by Pettini & Lipman (1995) and by van Zee et al. (1998) who have shown that both the neutral and ionized gas in I Zw 18 may have the same oxygen abundance.

New observations carried out with the *Far Ultraviolet Spectroscopic Explorer* (*FUSE*) by Vidal-Madjar et al.

¹ Using the customary definition $[\text{X}/\text{H}] = \log[N(\text{X})/N(\text{H})] - \log[N(\text{X})/N(\text{H})]_{\odot}$, and solar abundances from Grevesse et al. (1996) except for Ar for which the weighted average value -5.48 ± 0.04 from Sofia & Jenkins (1998) is adopted.

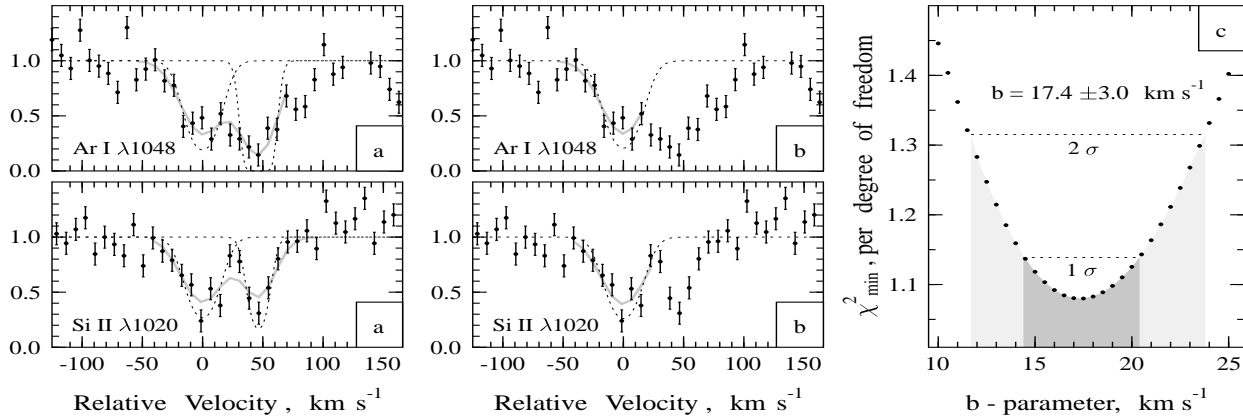


Fig. 1. (a) – Observed normalized intensities (dots with error bars) vs radial velocities from *FUSE* spectra of Ar I (top panel) and Si II (bottom panel) obtained by Vidal-Madjar et al. (2000). Smooth grey lines are the synthetic spectra (convolved with the spectrograph function) of the two-component microturbulent model calculated from the χ^2 minimization as described in the text. Smooth dotted lines show the corresponding unconvolved spectra. Components at $\Delta v \simeq 49$ km s $^{-1}$ are the Galactic H $_2$ lines [L(4-0)P(1) in top panel and L(7-0)P(4) in bottom panel] from the high-velocity cloud at -160 km s $^{-1}$. (b) – Same as **a** but for a one-component microturbulent model. (c) – Confidence regions in the $\chi^2_{\min} - b$ plane calculated from the simultaneous fit of the Ar I and Si II lines shown in panels **b**. The parabola vertex corresponds to the best value of $b = 17.4$ km s $^{-1}$

(2000) produce a similar puzzle : the column density ratio deduced from the Ar I $\lambda 1048$ and Si II $\lambda 1020$ lines in the neutral gas, $\log(\text{Ar}/\text{Si}) = -1.32$, differs significantly from that observed in the H II regions, $\log(\text{Ar}/\text{Si})_{\text{NW}} = -0.61 \pm 0.22$ and $\log(\text{Ar}/\text{Si})_{\text{SE}} = -0.74 \pm 0.22$ (Izotov et al. 2000). Izotov et al. suggested that ionization in DLAs may affect abundance ratios. To interpret the observations, they suggested a model consisting of two regions with *substantially different* metal contents, i.e. implicitly recalling an idea of the existence of two media in BCGs (a pristine gas, unprocessed since the big bang and a gas polluted by nucleosynthetic products – Kunth & Sargent 1986). In general, the discovery of such a primordial gas would be of great importance for cosmology, as noted by Kunth et al. (1994).

In this Letter, we report on the study of the Ar I $\lambda 1048$ and Si II $\lambda 1020$ profiles of I Zw 18 published by Vidal-Madjar et al. (2000). We show that these lines can be modeled under the assumption that the metal content in the neutral gas is the same as in the H II regions without referring to an ionization correction.

2. Data analysis and results

Spectroscopic observations of I Zw 18 with *FUSE* in the range $\sim 980 - 1187$ Å are described in detail by Vidal-Madjar et al. (2000). The spectrum was obtained with a resolution of about $\lambda/\Delta\lambda \sim 10,000$ and a signal-to-noise ratio of $S/N \sim 10$ per resolution element. The large entrance aperture ($30'' \times 30''$) fully covers the galactic surface ($\sim 10'' \times 4''$). As noted by Vidal-Madjar et al., *FUSE* produces the average absorption over the full body of the

galaxy. In this case the analysis of saturated absorption lines is not an easy and unambiguous task. The main difficulty is connected with the line broadening by large-scale irregular (stochastic) velocity fields. The influence of the finite correlation length on the line profile depends on the details of the observation. If one considers the line formation process in the light of a point source, then the observed spectrum reflects only one realization of the velocity field and, hence, large deviations from the expectation value of the intensity $\langle I_\lambda \rangle$ may occur if the correlation length of the velocity field ℓ is not very small compared to the size of the absorbing region (Levshakov & Kegel 1997). If, however, the spectrograph aperture covers an essential part of the galactic surface, then $\langle I_\lambda \rangle$ should reasonably well correspond to the observations. But also in this case the standard Voigt-fitting analysis (based on the assumption of microturbulence) may yield misleading results (Levshakov & Kegel 1994). Below we demonstrate this effect using the published *FUSE* data.

2.1. A microturbulent approach

We begin with the standard Voigt-fitting analysis which assumes a completely uncorrelated velocity field, i.e. $\ell = 0$ (*microturbulence*). In our example we use the published data from Fig. 1 of Vidal-Madjar et al. to illustrate how the column density ratio deduced from two lines, Ar I and Si II, is affected by the underlying assumptions. From these data given in arbitrary units we have calculated normalized intensities using the plotted synthetic profiles, and then added to the normalized data 1σ error bars corresponding to $S/N = 10$ (dots and error bars in Figs. 1a,

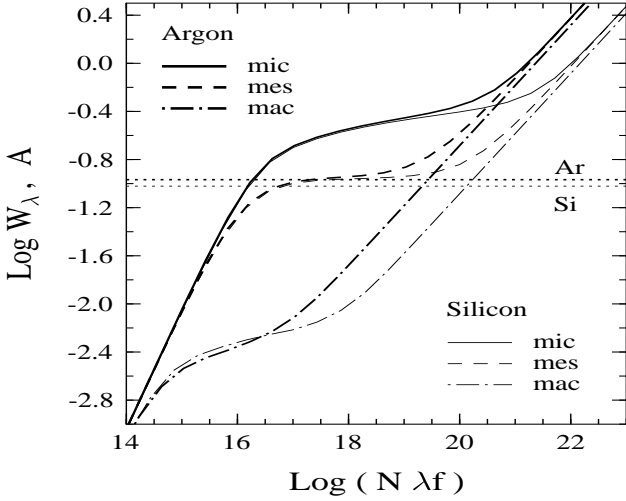


Fig. 2. Curves of growth for Ar I $\lambda 1048$ and Si II $\lambda 1020$ calculated with the fixed values of the velocity dispersion $\sigma = 13 \text{ km s}^{-1}$ and the kinetic temperature $T_{\text{kin}} = 200 \text{ K}$. Three types of lines correspond to micro-, meso-, and macroturbulence ($\ell = 0$, $L/\ell = 1.45$, $L/\ell = 0$, respectively). Dotted horizontal lines mark the estimated values of the Ar I and Si II equivalent widths

1b). Both profiles were centered at $v = 0 \text{ km s}^{-1}$ according to the synthetic spectra of Vidal-Madjar et al., and the internal uncertainty of our velocity scale calibration was estimated to be about $\pm 5 \text{ km s}^{-1}$.

The oscillator strengths of the Ar I $\lambda 1048.2119 \text{ \AA}$ and Si II $\lambda 1020.6989 \text{ \AA}$ lines, $f_{\text{Ar I}} = 0.257$ and $f_{\text{Si II}} = 0.01391$, were taken from Federman et al. (1992) and from Charro & Martín (2000), respectively.

The absorption lines of Ar I and Si II are partly blended with the Galactic H₂ L(4-0)P(1) and L(7-0)P(4) lines, respectively. To estimate the Ar I and Si II column densities and the b -parameter, we firstly fitted two component Voigt profiles to the observed intensities via χ^2 minimization. In this procedure the theoretical profiles were convolved with the instrumental point-spread function which is supposed to be a Gaussian with the width of 26 km s^{-1} . The best fit with $\chi_{\text{min}}^2 = 34.25$ ($M = 35$ data points, and $\nu = 28$ degrees of freedom) is shown in Fig. 1a by grey solid curves which simultaneously mark the data points involved in the optimization procedure. Dotted curves in Fig. 1a show the corresponding unconvolved profiles. As seen from this figure, the H₂ blends do not affect the cores of the Ar I and Si II lines much. This is why in the further analysis we used only the blue wings and the central parts of these lines.

Our main results are shown in Figs. 1b and 1c. Fig. 1b presents the best fit with $\chi_{\text{min}}^2 = 18.36$ ($M = 19$, $\nu = 16$), $N_{\text{Ar I}} = 6.83 \times 10^{13} \text{ cm}^{-2}$, $N_{\text{Si II}} = 1.11 \times 10^{15} \text{ cm}^{-2}$, and $b = 17.4 \text{ km s}^{-1}$. Fig. 1c shows the calculated χ_{min}^2 values as a function of b with the 1σ and 2σ confidence levels.

Table 1. Ar and Si abundances of neutral gas in I Zw 18

L/ℓ	$N_{\text{Si II}}, \text{ cm}^{-2}$	Ar/Si [‡]	$\frac{1}{\nu} \chi_{\text{min}}^2$	[Ar/H] [†]	[Si/H] [†]
0	1.0(19)	-1.93	1.33	1.03	1.91
0.50	4.4(18)	-1.82	1.13	0.77	1.11
0.75	1.6(18)	-1.57	1.08	0.58	1.11
0.90	4.1(17)	-1.12	1.06	0.43	0.51
1.00	4.9(16)	-0.32	1.06	0.31	-0.41
1.10	1.3(16)	0.07	1.07	0.14	-0.98
1.15	9.5(15)	0.10	1.07	0.02	-1.12
1.20	7.5(15)	0.02	1.07	-0.17	-1.22
1.25	6.3(15)	-0.05	1.08	-0.32	-1.30
1.30	5.4(15)	-0.34	1.08	-0.66	-1.36
1.35	5.0(15)	-0.71	1.08	-1.08	-1.40
1.40	4.4(15)	-0.75	1.08	-1.17	-1.46
1.45	4.0(15)	-0.84	1.08	-1.30	-1.50
1.50	3.7(15)	-0.90	1.08	-1.39	-1.53
2.00	2.5(15)	-1.09	1.08	-1.76	-1.71
5.00	1.5(15)	-1.19	1.08	-2.09	-1.94
10.0	1.3(15)	-1.20	1.08	-2.17	-2.00
∞	1.1(15)	-1.21	1.09	-2.23	-2.06

[‡] Ar/Si $\equiv \log(N_{\text{Ar I}}/N_{\text{Si II}})$

[†] the internal accuracy of these values is $\simeq 0.1$ dex

Here, for each point we fixed the value of b and minimize χ^2 by varying all other parameters.

The estimated ratio of $\log(\text{Ar/Si}) = -1.21$ is consistent within the uncertainty interval of 0.11 dex with the value -1.32 cited by Izotov et al. (2000). The most likely value for b , $17.4 \pm 3 \text{ km s}^{-1}$, is in an excellent agreement with the radio observations of the H I gas in I Zw 18 carried out by van Zee et al. (1998). The fact that $b_{\text{H I}} \simeq b_{\text{Ar I}}$ implies that the kinetic temperature of the neutral gas in I Zw 18 is less than 600 K and that the line broadening is caused mainly by turbulent motions.

To summarize this section we note that the microturbulent results lead to the puzzle mentioned above which encouraged us to try a more general model.

2.2. A mesoturbulent approach

21 cm observations with high spatial resolution show that the line profile varies with position (van Zee et al. 1998). This is a clear indication that large-scale motions determine the line profiles and that the microturbulent approach is not well founded. We therefore generalize our analysis to include the effects of a finite correlation length, i.e. $\ell \neq 0$ (mesoturbulence) and to study the limiting case $L/\ell \rightarrow 0$ (macroturbulence).

The simulation of the mesoturbulent Ar I and Si II profiles has been carried out using the simplified model of a plane-parallel slab of geometrical size L with homogeneous turbulence and uniform kinetic temperature, T_{kin} . Specifying the Ar I and Si II column densities, the L/ℓ ratio, the velocity dispersion σ , and the thermal widths for each line, we can calculate their average absorption-line

profiles employing the generalized radiative transfer equation (Levshakov & Kegel 1994, 1997).

The same χ^2 -minimization procedure as before was applied to the same data set, but now with two fitting parameters $\{N_{\text{Si II}}, \log(\text{Ar}/\text{Si})\}$, i.e. $\nu = 17$. We fixed $\sigma = 13 \text{ km s}^{-1}$ and $T_{\text{kin}} = 200 \text{ K}$ (i.e. $b \simeq 18 \text{ km s}^{-1}$) and calculated χ_{min}^2 for a given L/ℓ . The results are presented in Table 1. It should be emphasized that all Ar I and Si II profiles corresponding to the listed – very different – solutions are *identical* to those shown in Fig. 1b.

Our numerical results show that accounting for correlation effects strongly affects the derived column densities as well as the abundance ratio Ar/Si. These effects are closely related to the changes in the curves of growths caused by the finite L/ℓ value. Fig. 2 shows three curves of growth for each of the two lines. They correspond to the two limiting cases of micro- and macroturbulence (Gail et al. 1974), as well as to an intermediate – mesoturbulent – case ($L/\ell = 1.45$). In general, one may say that the column density derived from a measured equivalent width increases with increasing correlation length ℓ . Fig. 2 also allows a qualitative interpretation of the Ar/Si ratio in dependence of L/ℓ . In the microturbulent limit both lines are still close to the linear part of the curve of growth, while in the mesoturbulent regime they lie on the flat part. Since the slope here is smaller than on the linear part, the Ar/Si ratio is larger. In the macroturbulent limit, both lines lie on the square root part. In this case the slope is again steeper and, more importantly, the two curves of growth are well separated from each other (due to the different damping constants), implying a lower Ar/Si ratio than in the mesoturbulent case. Thus, going from micro- to macroturbulence we expect the Ar/Si ratio at first to rise and, after going through a maximum, to decline again. From Fig. 2 we also see that in the macroturbulent limit the Ar/Si ratio is lower than in the microturbulent one.

3. Conclusions

We have shown that metal abundances derived from the absorption profiles of Ar I $\lambda 1048$ and Si II $\lambda 1020$, observed in the spectrum of the damped Ly α system I Zw 18 by Vidal-Madjar et al. (2000), become fully consistent with those derived from emission-line spectra of the H II regions by Izotov & Thuan (1999) and by Izotov et al. (1999), if correlations in the large-scale velocity field are accounted for. The adequacy of the obtained mesoturbulent solutions is supported by the fact that the derived velocity dispersion of the neutral gas, $\sigma \simeq 13 \text{ km s}^{-1}$, is in an excellent agreement with the H I 21 cm observations, $\sigma = 12 - 14 \text{ km s}^{-1}$ (van Zee et al. 1998). This implies that the gas in I Zw 18 is efficiently mixed.

To estimate more accurately metal abundances in the H I gas within the framework of our model, one needs to know the L/ℓ ratio. This parameter can be found from the analysis of saturated and optically thin lines of the same

ion, since the latter are less affected by the correlation effects. For our case, observations of the Ar I $\lambda 1066$ line would be of particular interest since its oscillator strength $f_{1066} = 1/4 f_{1048}$. The Ar I $\lambda 1066$ line was observed in the $z = 3.4$ DLA system toward the quasar Q0000-2620 and its analysis showed a remarkably similar abundance to the other α -chain elements O, S, and Si, $Z/Z_{\odot} \simeq 1/80$ (Molaro et al. 2000). The similarity of both DLA systems is also supported by the very low molecular hydrogen contents found in I Zw 18, $f(\text{H}_2) \equiv 2N_{\text{H}_2}/N_{\text{H I}} \ll 10^{-6}$ (Vidal-Madjar et al. 2000), and at $z = 3.4$, $f(\text{H}_2) \simeq 4 \times 10^{-8}$ (Levshakov et al. 2000).

Since Ar can hardly be depleted onto dust grains, but can be partially ionized by nearby UV stellar radiation with energies $h\nu > 15.76 \text{ eV}$, the relative abundance of Ar I is a good indicator of the intensity of the local photoionizing flux (Sofia & Jenkins 1998). Our measurements rule out the presence of a significant amount of partially ionized gas in the damped Ly α system I Zw 18 and, hence, metal abundances in the neutral gas do not require ionization corrections as suggested by Izotov et al. (2000).

Thus, it is extremely important in future observations to investigate low-ion lines to understand better the kinematic characteristics of the neutral gas bulk motion which will enable us to obtain more reliable estimations of metallicities.

Acknowledgements. The work of S.A.L. and I.I.A. is supported in part by the Deutsche Forschungsgemeinschaft and by the RFBR grant No. 00-02-16007.

References

- Charro E., Martín I. 2000, ApJS 126, 551
- Federman S. R., Beideck D. J. et al. 1992, ApJ 401, 367
- Gail H. P., Hundt E., Kegel W. H., Schmid-Burgk J., Traving G. 1974, A&A 32, 65
- Grevesse N., Noels A., Sauval A. J. 1996, in Cosmic Abundances ASP Conf. Series, Vol. 99, p. 117
- Izotov Yu. I., Thuan T. X. 1999, ApJ 511, 639
- Izotov Yu. I., Chaffee F. H. et al. 1999, ApJ 527, 757
- Izotov Yu. I., Schaerer D., Charbonnel C. 2000, ApJ, in press (astro-ph/0010643)
- Kunth D., Lequeux J., Sargent W. L. W., Viallefond F. 1994, A&A 282, 709
- Kunth D., Sargent W. L. W. 1986, ApJ 300, 496
- Levshakov S. A., Kegel W. H. 1994, MNRAS 271, 161
- Levshakov S. A., Kegel W. H. 1997, MNRAS 288, 787
- Levshakov S. A., Molaro P. et al. 2000, A&A 361, 803
- Molaro P., Levshakov S. A. et al. 2000, ApJ, in press (astro-ph/0010434)
- Östlin, G. 2000, ApJ 535, L99
- Pettini M, Lipman K. 1995, A&A 297, L63
- Sofia U. J., Jenkins E. B. 1998, ApJ 499, 951
- van Zee L., Westpfahl D. et al. 1998, AJ 115, 1000
- Vidal-Madjar A., Kunth D. et al. 2000, ApJ 538, L77
- Zwicky F. 1966, ApJ 143, 192